

Spontaneous decay of a two-level atom near the left-handed slab

Jing-Ping Xu,^{1,2,3} Ya-Ping Yang,² Qiang Lin,¹ and Shi-Yao Zhu^{1,2,3}

¹*Institute of Optics, Zhejiang University, Hangzhou 310027, China*

²*Department of Physics, Tongji University, Shanghai 200092, China*

³*Department of Physics, Hong Kong Baptist University, Hong Kong, China*

(Received 23 January 2009; published 14 April 2009)

Spontaneous decay of a two-level atom near the left-handed material (LHM) slab is investigated. The contributions of the guided modes and the surface-plasmon polariton (SPP) modes supported by the LHM slab to the spontaneous decay are studied at length. We find that the atomic decay near a LHM slab is much different from that near a dielectric slab or metal slab. The first—the dielectric slab with arbitrary thickness—supports at least two guided modes (one for TE polarized and one for TM polarized), but LHM slab may support none of the guided mode for certain thickness. The second—the atom near the LHM slab—may decay through both TE- and TM-polarized SPP, but the atom near the metal slab can decay only through TM-polarized SPP. The third, when the LHM slab supports only TE-polarized SPP modes, the atom near such slab cannot couple to the SPP mode when its dipole moment is perpendicular to the interface. Even if LHM contains weak loss, above analysis is also valid, and the decay rate directly related to material's losses (defined by the decay through dissipation here) can be distinguished from the total decay rate. Most interesting, we find that the decay through SPP will be larger than the decay through dissipation when the atom is placed at an appropriate position. Our results will give constructive reference to the design and fabrication of the quantum device made of LHM.

DOI: [10.1103/PhysRevA.79.043812](https://doi.org/10.1103/PhysRevA.79.043812)

PACS number(s): 42.50.Nn, 42.50.Lc, 42.25.Bs

I. INTRODUCTION

It is known that the atomic spontaneous decay depends on both properties of itself and surrounding environment [1]. Recently, the quantum effect of the atom in the structure containing left-handed materials (LHMs) [2] has attracted considerable attention [3–10]. The LHM possesses negative permittivity, permeability, and refractive index simultaneously. In the LHM, the wave vector is antiparallel to the direction of energy flow, so that the electric field, magnetic field, and the wave vector form a left-handed triplet. In 2003, Dung *et al.* [3] discussed the electromagnetic-field quantization and spontaneous decay in isotropic left-handed materials with real-cavity model. Ruppin and Martin [4] obtained the lifetime of an emitting dipole near interfaces of the LHM with a classical electromagnetic calculation. Kästel and Fleischhauer [5] found that an ideal LHM slab mounted on a perfect mirror can completely inhibit the spontaneous decay of a two-level atom when the atomic dipole is parallel to the interface. The influence of the absorption of the LHM on the spontaneous decay of the two-level atom was studied in [6,7]. The quantum interference of a Zeeman V-type atom in the cavity containing LHM [8] or one-dimensional photonic crystals containing LHM [9] was investigated. Van der Waals interaction and spontaneous decay of an excited atom in a superlenslike geometry was also studied in Ref. [10].

Most of the previous studies focused on the radiative decay [5–9]. Besides the radiative decay, they defined the other decay channels as nonradiative channels due to the losses roughly [3,4,7,8,10]. In this paper, we mainly consider the spontaneous decay of atom near the LHM slab and classify the decay channels into four kinds: decay through radiation, through guided mode, through surface-plasmon polariton (SPP) mode, and through dissipation due to losses of mate-

rials. We found that the spontaneous decay of atom near the LHM slab is much different from that near the dielectric slab and the metal slab due to the contribution of the guided mode and the SPP mode, and our result has potential application in single-photon source and other quantum devices.

This paper is organized as follows. In Sec. II, we introduce the model and the interaction Hamiltonian. The formula of decay rates of a two-level atom near LHM slab is given in Sec. III. The numerical calculations have been performed in Sec. IV. Finally we give the conclusion in Sec. V.

II. MODEL AND INTERACTION HAMILTONIAN

The space structure is plotted in Fig. 1, which the left-handed slab is marked by “M” with indices ϵ_M , μ_M , n_M , and thickness d , and its left and right semi-infinite dielectrics are vacuum, i.e., $\epsilon_L = \epsilon_R = \epsilon_0$ and $\mu_L = \mu_R = \mu_0$. The absolute value of the refractive indexes of the LHM is larger than that of the vacuum. Interfaces are in the x - y plane, and the origin of the z coordinate is taken at the left interface of layer M.

Here we adopt the quantization method used in Refs. [3,7–9], which is suitable for both loss and lossless cases to study the spontaneous decay of a two-level atom with the

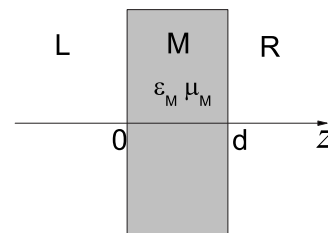


FIG. 1. Sketch of the structure we considered.

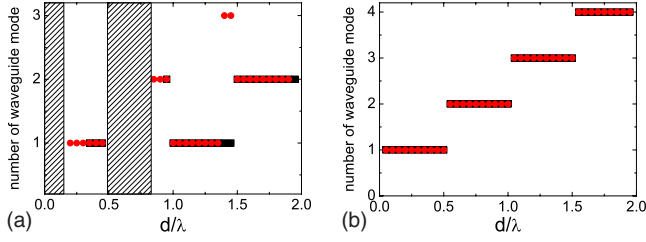


FIG. 2. (Color online) The number of guided mode as a function of thickness. (a) the LHM slab with $\epsilon_M = -2$ and $\mu_M = -1$; (b) the dielectric slab with $\epsilon_M = 2$ and $\mu_M = 1$. The black square refers to N_{TE} , while the red rotundity refers to N_{TM} . Here $\lambda = 2\pi c / \omega_0$ and the step of d is 0.05λ .

transition frequency ω_0 placed at arbitrary position on the z axis $\mathbf{r}_a = (0, 0, z_a)$. Following Ref. [3], the Hamiltonian of the whole system under the rotation wave approximation can be written as

$$\hat{H} = \sum_{\lambda=e,m} \int d^3\mathbf{r} \int_0^\infty d\omega \hbar \omega \hat{f}_\lambda^\dagger(\mathbf{r}, \omega) \cdot \hat{f}_\lambda(\mathbf{r}, \omega) + \hbar \omega_0 \hat{\sigma}_z - \left[\hat{\sigma}^+ \mathbf{P}_a \cdot \int_0^\infty d\omega \hat{\mathbf{E}}(\mathbf{r}_a, \omega) + \text{H.c.} \right], \quad (1)$$

where $\hat{f}_\lambda^\dagger(\mathbf{r}, \omega)$ and $\hat{f}_\lambda(\mathbf{r}, \omega)$ are the fundamental vector operators of the environment composed of the electromagnetic field and the medium [3], and the subscript $\lambda = e, m$ denotes the electric and the magnetic excitons. The operators satisfy the following commutation relations:

$$[\hat{f}_{\lambda i}(\mathbf{r}, \omega), \hat{f}_{\lambda' j}^\dagger(\mathbf{r}', \omega')] = \delta_{\lambda\lambda'} \delta_{ij} \delta(\mathbf{r} - \mathbf{r}') \delta(\omega - \omega'), \quad (2)$$

$$[\hat{f}_{\lambda i}(\mathbf{r}, \omega), \hat{f}_{\lambda' i}^\dagger(\mathbf{r}', \omega')] = 0, \quad (3)$$

where $i, j = x, y, z$ are three orthogonal components in Cartesian coordinates. In Eq. (1), $\hat{\sigma} = |l\rangle\langle u|$ and $\hat{\sigma}^+ = |u\rangle\langle l|$ are the Pauli operators of the two-level atom. Here $|l\rangle$ and $|u\rangle$ mean that the atom is in the lower and upper levels, respectively. $\mathbf{P}_a = \langle l | \hat{\mathbf{P}}_a | u \rangle = \langle u | \hat{\mathbf{P}}_a | l \rangle$ is the transition dipole moment. The electric field operator satisfies the following equation [3]:

$$\nabla \times \frac{1}{\mu(\mathbf{r}, \omega)} \nabla \times \hat{\mathbf{E}}(\mathbf{r}, \omega) - \frac{\omega^2}{c^2} \epsilon(\mathbf{r}, \omega) \hat{\mathbf{E}}(\mathbf{r}, \omega) = i\omega\mu_0 \hat{\mathbf{j}}_N(\mathbf{r}, \omega). \quad (4)$$

Here $\hat{\mathbf{j}}_N(\mathbf{r}', \omega)$ is the noise current operator, which can be expressed by the fundamental operators as [3]

$$\hat{\mathbf{j}}_N(\mathbf{r}, \omega) = \omega \sqrt{\frac{\hbar \epsilon_0}{\pi}} \text{Im} \epsilon(\mathbf{r}, \omega) \hat{\mathbf{f}}_e(\mathbf{r}, \omega) + \nabla \times \sqrt{-\frac{\hbar}{\pi \mu_0} \text{Im} \frac{1}{\mu(\mathbf{r}, \omega)}} \hat{\mathbf{f}}_m(\mathbf{r}, \omega). \quad (5)$$

The solution of Eq. (4) can be formally written as

$$\hat{\mathbf{E}}(\mathbf{r}, \omega) = i\omega\mu_0 \int d^3\mathbf{r}' \vec{\mathbf{G}}(\mathbf{r}, \mathbf{r}', \omega) \cdot \hat{\mathbf{j}}_N(\mathbf{r}', \omega), \quad (6)$$

where $\vec{\mathbf{G}}(\mathbf{r}, \mathbf{r}', \omega)$ is the classical Green's tensor satisfying the equation

$$\nabla \times \frac{1}{\mu(\mathbf{r}, \omega)} \nabla \times \vec{\mathbf{G}}(\mathbf{r}, \mathbf{r}', \omega) - \frac{\omega^2}{c^2} \epsilon(\mathbf{r}, \omega) \vec{\mathbf{G}}(\mathbf{r}, \mathbf{r}', \omega) = \delta(\mathbf{r} - \mathbf{r}'). \quad (7)$$

The wave function of the whole system at time t is

$$|\psi(t)\rangle = C_u(t) e^{-i\omega_0 t} |u, 0\rangle + \sum_{\lambda=e,m} \int d^3\mathbf{r} \int_0^\infty d\omega e^{-i\omega t} C_{\lambda l}(\mathbf{r}, \omega, t) \cdot |l, \mathbf{I}_\lambda(\mathbf{r}, \omega)\rangle, \quad (8)$$

where the state vector $|u, 0\rangle$ describes the atom in the upper level with no exciton, and the state vector $|l, \mathbf{I}_\lambda(\mathbf{r}, \omega)\rangle$ represents the atom in the lower level with one exciton of $\mathbf{I}_\lambda(\mathbf{r}, \omega)$, i.e., $\hat{f}_\lambda^\dagger(\mathbf{r}, \omega)|0\rangle = |\mathbf{I}_\lambda(\mathbf{r}, \omega)\rangle$.

The atom is prepared in the upper level initially. Inserting Eqs. (1) and (8) into the Schrödinger equation, the dynamic equation of atomic upper-level amplitude can be obtained under the Markovian approximation,

$$\begin{aligned} \dot{C}_u(t) &= -\frac{1}{2} C_u(t) \left[\frac{2}{\epsilon_0 \hbar} \frac{\omega_0^2}{c^2} \mathbf{P}_a \cdot \text{Im} \vec{\mathbf{G}}(\mathbf{r}_a, \mathbf{r}_a, \omega_0) \cdot \mathbf{P}_a \right] \\ &= -\frac{1}{2} \Gamma C_u(t), \end{aligned} \quad (9)$$

where $\text{Im} \vec{\mathbf{G}}(\mathbf{r}_a, \mathbf{r}_a, \omega_0)$ is the imaginary part of the classical Green's tensor at frequency ω_0 and position \mathbf{r}_a . The atomic dipole moment can be parallel to the interface (along the x axis and denoted by \parallel) and perpendicular to the interface (along the z axis and denoted by \perp). With the Green's tensor in hand (see Appendix A), we get the formula of spontaneous decay rate of an atom at arbitrary position as [7]

(i) The atom is placed in the left region ($z_a \leq 0$),

$$\begin{aligned} \Gamma_{\parallel \text{Total}}(z_a) &= \frac{3}{4} \Gamma_0 \text{Re} \mu_L n_L \int_0^\infty \frac{dK_{\parallel}}{K_L} \frac{K_{\parallel}}{K_{Lz}} \\ &\times \left\{ \left[1 + \frac{r_{LM}^{\text{TE}} + r_{MR}^{\text{TE}} e^{2iK_{Mz}d}}{D_{\text{TE}}} e^{-i2K_{Lz}z_a} \right] \right. \\ &\left. + \frac{K_{Lz}^2}{K_L^2} \left[1 - \frac{r_{LM}^{\text{TM}} + r_{MR}^{\text{TM}} e^{2iK_{Mz}d}}{D_{\text{TM}}} e^{-2iK_{Lz}z_a} \right] \right\}, \end{aligned} \quad (10a)$$

$$\begin{aligned} \Gamma_{\perp \text{Total}}(z_a) &= \frac{3}{2} \Gamma_0 \text{Re} \mu_L n_L \int_0^\infty \frac{dK_{\parallel}}{K_{Lz}} \frac{K_{\parallel}^3}{K_L^3} \\ &\times \left[1 + \frac{r_{LM}^{\text{TM}} + r_{MR}^{\text{TM}} e^{2iK_{Mz}d}}{D_{\text{TM}}} e^{-2iK_{Lz}z_a} \right]. \end{aligned} \quad (10b)$$

(ii) The atom is placed in the middle slab ($0 < z_a \leq d$),

$$\Gamma_{\parallel \text{Total}}(z_a) = \frac{3}{4}\Gamma_0 \text{Re} \mu_M n_M \int_0^\infty \frac{dK_{\parallel}}{K_M K_{Mz}} \left\{ \left[1 + \frac{2r_{ML}^{\text{TE}} r_{MR}^{\text{TE}} e^{2iK_{Mz}d} + r_{ML}^{\text{TE}} e^{2iK_{Mz}z_a} + r_{MR}^{\text{TE}} e^{2iK_{Mz}(d-z_a)}}{D_{\text{TE}}} \right] + \frac{K_{Mz}^2}{K_M^2} \left[1 + \frac{2r_{ML}^{\text{TM}} r_{MR}^{\text{TM}} e^{2iK_{Mz}d} - r_{ML}^{\text{TM}} e^{2iK_{Mz}z_a} - r_{MR}^{\text{TM}} e^{2iK_{Mz}(d-z_a)}}{D_{\text{TM}}} \right] \right\}, \quad (11a)$$

$$\Gamma_{\perp \text{Total}}(z_a) = \frac{3}{2}\Gamma_0 \text{Re} \mu_M n_M \int_0^\infty \frac{dK_{\parallel}}{K_{Mz} K_M^3} \left[1 + \frac{2r_{ML}^{\text{TM}} r_{MR}^{\text{TM}} e^{2iK_{Mz}d} + r_{ML}^{\text{TM}} e^{2iK_{Mz}z_a} + r_{MR}^{\text{TM}} e^{2iK_{Mz}(d-z_a)}}{D_{\text{TM}}} \right]. \quad (11b)$$

Because the structure is symmetry, the decay rate of atom in the right region ($z_a \geq d$) has the same value as that in the left region. Here $K_i = n_i K_0 = n_i \omega_0 / c$ ($i = L, M, R$), K_{\parallel} is the component of wave vector parallel to the interface, K_{iz} is the z component of wave vector in the i th region, and they relate to each other through $K_{\parallel}^2 + K_{iz}^2 = K_i^2$, $\Gamma_0 = p_a^2 \omega_0^3 / (3\pi \epsilon_0 \hbar c^3)$ is the decay rate in free space. The coefficient $r_{ML}^{\text{TE/TM}}$ is the reflection coefficient of the electromagnetic field incident from M to L for TE/TM polarization and $r_{MR}^{\text{TE/TM}}$ is the reflection coefficient from M to R for TE/TM polarization, which

$$r_{ML/R}^{\text{TE}} = \frac{\mu_{L/R} K_{Mz} - \mu_M K_{L/Rz}}{\mu_{L/R} K_{Mz} + \mu_M K_{L/Rz}}, \quad (12)$$

$$r_{ML/R}^{\text{TM}} = \frac{\epsilon_{L/R} K_{Mz} - \epsilon_M K_{L/Rz}}{\epsilon_{L/R} K_{Mz} + \epsilon_M K_{L/Rz}}. \quad (13)$$

$D_{\text{TE/TM}}$ originates from the multireflection effect and has the form

$$D_{\lambda} = 1 - r_{ML}^{\lambda} r_{MR}^{\lambda} e^{2iK_{Mz}d}. \quad (14)$$

III. ANALYSIS OF SPONTANEOUS DECAY

A. Decay through radiation

Decay through radiation refers to that of the atom transits from the upper level down to the lower level through emitting a propagating photon. Because $n_R = n_L = 1 < |n_M|$, the decay through radiation is embodied by the integration over K_{\parallel} from 0 to $n_L K_0$ in Eqs. (10) and (11). Because this kind of decay in various environments had been studied in many previous works [4–9], we do not discuss it in detail and only note that $K_{Mz} = -\sqrt{\epsilon_M \mu_M K_0^2 - K_{\parallel}^2}$ if layer M is made of the left-handed materials, while $K_{Mz} = \sqrt{\epsilon_M \mu_M K_0^2 - K_{\parallel}^2}$ if layer M is dielectric.

B. Decay through guided modes

The guided modes refer to modes which are evanescent waves in the two semi-infinite regions and standing waves in layer M . The guided modes exist when K_{\parallel} falls into the region $(n_L K_0, |n_M| K_0)$, where K_{Lz} and K_{Rz} become pure imaginary and K_{Mz} is real. According to the Maxwell equations and the boundary condition, the guided modes only occur at discrete propagation constant K_{\parallel} leading to $D_{\text{TE}}=0$ for TE

polarization and $D_{\text{TM}}=0$ for TM polarization [11–13].

If $D_{\text{TE/TM}}=0$, the integrands in Eqs. (10) and (11) are divergent; thereby the decay rate related to the guided mode can be calculated through several methods, such as renormalizing the density of mode [13] and the residue theorem for the pole [11,12]. Here we adopt the residue theorem for the pole to obtain the decay rate of atom with dipole moment parallel to the interface through guided mode. (The formula for atomic dipole normal to the interface can be obtained with the similar method.)

For $z_a \leq 0$, we have

$$\begin{aligned} \Gamma_{\parallel \text{WG}}(z_a) = & \frac{3}{4}\Gamma_0 \text{Re} u_L \sum_{j=1}^{N_{\text{TE}}} \frac{K_{\parallel j}}{K_{Lzj}} \pi i (r_{LM}^{\text{TE}} + r_{MR}^{\text{TE}} e^{2iK_{Mzj}d}) \\ & \times \left(\frac{\partial D_{\text{TE}}}{\partial K_{\parallel}} \bigg|_{K_{\parallel}=K_{\parallel j}} \right)^{-1} e^{-i2K_{Lzj}z_a} \\ & - \frac{3}{4}\Gamma_0 \text{Re} u_L \sum_{g=1}^{N_{\text{TM}}} \frac{K_{\parallel g} K_{Lzg}}{n_L^2 K_0^2} \pi i (r_{LM}^{\text{TM}} + r_{MR}^{\text{TM}} e^{2iK_{Mzg}d}) \\ & \times \left(\frac{\partial D_{\text{TM}}}{\partial K_{\parallel}} \bigg|_{K_{\parallel}=K_{\parallel g}} \right)^{-1} e^{-i2K_{Lzg}z_a}, \end{aligned} \quad (15)$$

and for $0 < z_a \leq d$, we have

$$\begin{aligned} \Gamma_{\parallel \text{WG}}(z_a) = & \frac{3}{4}\Gamma_0 \text{Re} u_M \sum_{j=1}^{N_{\text{TE}}} \frac{K_{\parallel j}}{K_{Mzj}} \pi i [2 + r_{ML}^{\text{TE}} e^{i2K_{Mzj}z_a} \\ & + r_{MR}^{\text{TE}} e^{i2K_{Mzj}(d-z_a)}] \left(\frac{\partial D_{\text{TE}}}{\partial K_{\parallel}} \bigg|_{K_{\parallel}=K_{\parallel j}} \right)^{-1} \\ & + \frac{3}{4}\Gamma_0 \text{Re} u_M \sum_{g=1}^{N_{\text{TM}}} \frac{K_{\parallel g} K_{Mzg}}{n_M^2 K_0^2} \pi i [2 - r_{ML}^{\text{TM}} e^{i2K_{Mzg}z_a} \\ & - r_{MR}^{\text{TM}} e^{i2K_{Mzg}(d-z_a)}] \left(\frac{\partial D_{\text{TM}}}{\partial K_{\parallel}} \bigg|_{K_{\parallel}=K_{\parallel g}} \right)^{-1}, \end{aligned} \quad (16)$$

where $K_{\parallel j}$ and $K_{\parallel g}$ represent the propagation constants of the guided modes for TE and TM polarizations, respectively. To get the above decay rates, $K_{\parallel j}$ or $K_{\parallel g}$ can be identified as the first-order pole of the integrand, and the residue number can be achieved by replacing $D_{\text{TE/TM}}$ in Eqs. (10) and (11) by $\partial D_{\text{TE/TM}} / \partial K_{\parallel}$ [11,12]. The integers N_{TE} and N_{TM} are the numbers of the guided modes for TE and TM polarizations.

In the case of the dielectric slab, the analysis expression of N_{TE} and N_{TM} are [13]

$$N_{TE} = 1 + \left[\frac{K_0 d}{\pi} \sqrt{n_M^2 - n_L^2} - \frac{1}{\pi} \arctan \left(\frac{\mu_M \sqrt{n_L^2 - n_R^2}}{\mu_R \sqrt{n_M^2 - n_L^2}} \right) \right], \quad (17)$$

$$N_{TM} = 1 + \left[\frac{K_0 d}{\pi} \sqrt{n_M^2 - n_L^2} - \frac{1}{\pi} \arctan \left(\frac{\varepsilon_M \sqrt{n_L^2 - n_R^2}}{\varepsilon_R \sqrt{n_M^2 - n_L^2}} \right) \right], \quad (18)$$

where $[\xi]$ denotes the largest integer that is smaller than or equal to ξ . It is clear that for the dielectric slab with , there always exists at least one guided mode for both TE and TM polarizations whenever the thickness is small or large.

However, for LHM slab, N_{TE} and N_{TM} for the LHM slab cannot be given analytically and can be calculated numerically. It should be noticed that N_{TE} or N_{TM} may be zero when the thickness of LHM slab is small (see Appendix B). For example, we set the indexes of the dielectric slab are $\varepsilon_M = 2$, $\mu_M = 1$, while the indexes of the LHM slab are $\varepsilon_M = -2$, $\mu_M = -1$. Note that $K_{MZ} = -\sqrt{\varepsilon_M \mu_M K_0^2 - K_{||}^2}$ for the LHM slab, while $K_{MZ} = \sqrt{\varepsilon_M \mu_M K_0^2 - K_{||}^2}$ for the dielectric slab. N_{TE} and N_{TM} varying with thickness of the slab are shown in Fig. 2.

From Fig. 2, the number of the guided mode for the LHM slab is much different from that for the dielectric slab. N_{TE} and N_{TM} for the dielectric slab increase monotonously with thickness in a form of a ladder. However, for LHM slab, though N_{TE} and N_{TM} increase with thickness in general, they accompany with fluctuation. Note that for the LHM slab in Fig. 2(a), there is none of the guided mode for both TE and TM polarizations in the region of thickness $[0, 0.15\lambda]$ and $[0.5\lambda, 0.85\lambda]$ [see the spare shade in Fig. 2(a)].

C. Decay through the surface-plasmon polariton modes

The SPP mode refers to the electromagnetic mode which propagates along the interface and exponentially decays away from the interface in all three regions [14]. SPP has promising applications on fabricating plasmonic chips, plasmonic couplers, plasmonic modulators, plasmonic nanolithography, and plasmonic light sources. SPP near the metal surface had been studied at length over several decades [11,12]. Recently, SPPs near semi-infinite LHM [15] and LHM slab [16] has also been found. Different from the metal surface where only TM-polarized SPPs exist, both TM- and TE-polarized SPP modes can occur near the surface of LHM. The reason is that negative permittivity and negative permeability of LHM provide TE- and TM-polarized SPP modes, respectively, satisfying the Maxwell equation and boundary condition. Although the classical properties of the SPP near LHM have been studied at length, the spontaneous decay of atom near LHM through the SPP is rarely mentioned.

The SPP mode can occur as $K_{||} > |n_M|K_0$ for the LHM slab and $K_{||} > n_L K_0$ for the metal slab but cannot exist for the dielectric slab. In the region of $K_{||}$ for SPP, $K_{MZ} = -i\sqrt{K_{||}^2 - \varepsilon_M \mu_M K_0^2}$ is negative pure imaginary in the LHM, but $K_{MZ} = i\sqrt{K_{||}^2 - \varepsilon_M \mu_M K_0^2}$ is positive pure imaginary in the

metal. In other words, the amplitude of evanescent wave decreases as far away from the source in the metal but increases as far away from the source in the LHM. Similar to guided modes, the excitation condition of the SPP mode is also $D_{TE}=0$ for TE polarization and $D_{TM}=0$ for TM polarization.

The propagation constant of SPP $K_{||}$ satisfying $D_{TE}=0$ or $D_{TM}=0$ is also the first-order pole of integrand in Eqs. (10) and (11). So the corresponding decay rates can be achieved with the residue theorem similarly. The decay rates through the SPP mode have the same formation with that through the guided mode except that K_{MZ} is pure imaginary for SPP.

For $z_a \leq 0$, we have

$$\begin{aligned} \Gamma_{||SPP}(z_a) = & \frac{3}{4} \Gamma_0 \operatorname{Re} u_L \sum_{j=1}^{M_{TE}} \frac{K_{||j}}{K_{LZj}} \pi i (r_{LM}^{TE} + r_{MR}^{TE} e^{2iK_{MZj}d}) \\ & \times \left(\frac{\partial D_{TE}}{\partial K_{||}} \bigg|_{K_{||}=K_{||j}} \right)^{-1} e^{-2iK_{LZj}z_a} \\ & - \frac{3}{4} \Gamma_0 \operatorname{Re} u_L \sum_{g=1}^{M_{TM}} \frac{K_{||g} K_{LZg}}{n_M^2 K_0^2} \pi i (r_{LM}^{TM} + r_{MR}^{TM} e^{2iK_{MZg}d}) \\ & \times \left(\frac{\partial D_{TM}}{\partial K_{||}} \bigg|_{K_{||}=K_{||g}} \right)^{-1} e^{-2iK_{LZg}z_a}, \end{aligned} \quad (19)$$

and for $0 < z_a \leq d$, we have

$$\begin{aligned} \Gamma_{||SPP}(z_a) = & \frac{3}{4} \Gamma_0 \operatorname{Re} u_M \sum_{j=1}^{M_{TE}} \frac{K_{||j}}{K_{MZj}} \pi i [2 + r_{ML}^{TE} e^{2iK_{MZj}z_a} \\ & + r_{MR}^{TE} e^{2iK_{MZj}(d-z_a)}] \left(\frac{\partial D_{TE}}{\partial K_{||}} \bigg|_{K_{||}=K_{||j}} \right)^{-1} \\ & + \frac{3}{4} \Gamma_0 \operatorname{Re} u_M \sum_{g=1}^{M_{TM}} \frac{K_{||g} K_{MZg}}{n_M^2 K_0^2} \pi i [2 - r_{ML}^{TM} e^{2iK_{MZg}z_a} \\ & - r_{MR}^{TM} e^{2iK_{MZg}(d-z_a)}] \left(\frac{\partial D_{TM}}{\partial K_{||}} \bigg|_{K_{||}=K_{||g}} \right)^{-1} \end{aligned} \quad (20)$$

It should be noted that for arbitrary thickness, the number of TM-polarized SPP M_{TM} for metal slab is no larger than 2 and $M_{TE}=0$ [11,12]; while both M_{TE} and M_{TM} are no larger than 1 for the LHM slab [16]. It means that the maximum number of the SPP in the LHM slab equals to that of the metal slab. In Fig. 3, we plot the dispersion relation of the SPP varying with thickness in the metal and the LHM.

From Fig. 3(a), there are two TM-polarized SPP modes for the metal slab with certain thickness. When thickness is larger than 0.35λ , two TM-polarized SPP modes degenerate. There is none of SPP mode when thickness is larger than 0.92λ . For the LHM slab $\varepsilon_M = -2$, $\mu_M = -1$ in Fig. 3(b); only one TM-polarized SPP mode exists when $d < 0.2\lambda$ and only one TE-polarized SPP mode exists when $0.2 < d < 0.32\lambda$. Thereby, TE SPP mode cannot coexist with TM-polarized SPP for arbitrary thickness. If we set permittivity and permeability both deviating from -1 , i.e., $\varepsilon_M = -1.5$, $\mu_M = -1.2$ in Fig. 3(c), both TE- and TM-polarized SPP modes can coexist

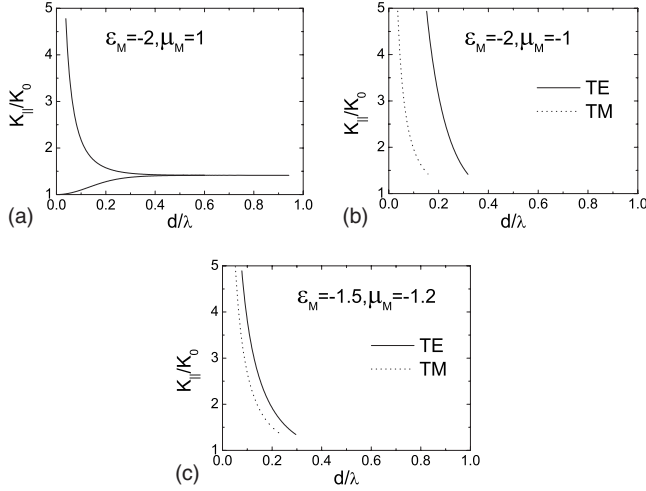


FIG. 3. The dispersion relations of SPP mode vary with the thickness. (a) The metal slab with $\epsilon_M = -2$ and $\mu_M = 1$; (b) the LHM slab with $\epsilon_M = -2$ and $\mu_M = -1$; (c) the LHM slab with $\epsilon_M = -1.5$ and $\mu_M = -1.2$.

for $0.09\lambda < d < 0.22\lambda$. However, the number of SPP mode cannot exceed two. It should be noticed that the maximum thickness supporting the SPP mode in the LHM slab is much shorter than that in the corresponding metal slab; this means that the mode volume of the SPP for the LHM is much smaller than that for corresponding metal, if the SPP mode exists.

D. Decay through dissipation

This kind of decay occurs only if the middle slab contains losses. If the middle slab is made of transparent materials, i.e., ϵ_M and μ_M are both real, the decay through dissipation disappears. Here we restrict the cases which the imaginary part of ϵ_M or μ_M is much small. Under such condition, the decay through dissipation can be distinguished from the total decay, which is $\Gamma_{\text{Diss}} = \Gamma_{\text{Total}} - \Gamma_{\text{Rad}} - \Gamma_{\text{WG}} - \Gamma_{\text{SPP}}$, here Γ_{Total} is the numerical result of Eq. (10). When the middle slab contains losses, the spontaneous decay of atom embedded in it is much complicated because the modified factor of decay rate is dependent on the radius of real cavity surrounding the atom and cannot tend to a constant with the decreasing of radius [3]. In addition, if the real cavity is considered much small which is the order of the distance between constituent atoms of the middle slab, the slab cannot be identified as uniform materials. So, if the slab contains losses, we do not discuss the decay rate of atom embedded in middle slab here and only consider the cases of atom near the surface of slab.

IV. CALCULATION AND ANALYSIS

In this section, we calculate the atomic decay rates as function of the position for different materials. We omit the near field effect when the atom is embedded in middle slab because it can be normalized easily by the decay rate in corresponding infinite materials.

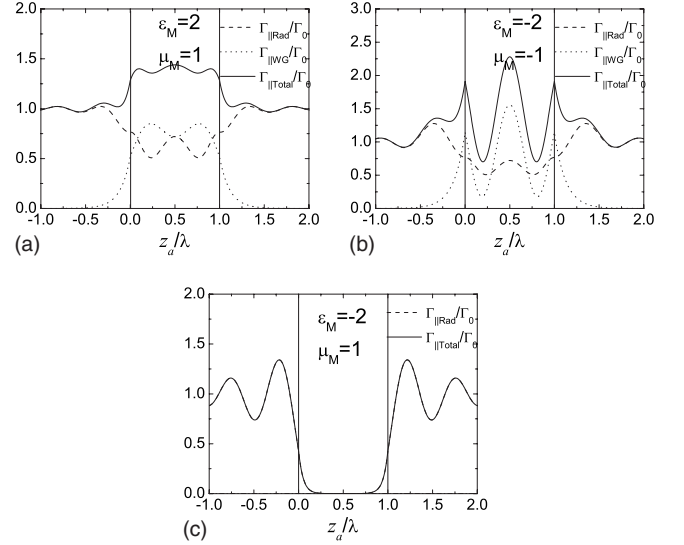


FIG. 4. The decay rates as functions of the atomic position when the thicknesses of slab are $d = \lambda$ and the atomic dipole is parallel to interface. (a) The dielectric slab with $\epsilon_M = 2$ and $\mu_M = 1$, (b) the LHM slab with $\epsilon_M = -2$ and $\mu_M = -1$, and (c) the metal slab with $\epsilon_M = -2$ and $\mu_M = 1$.

A. Transparent slab

We will compare the case of dielectric slab of $\epsilon_M = 2$ and $\mu_M = 1$, the case of LHM slab of $\epsilon_M = -2$ and $\mu_M = -1$, and the case of metal slab of $\epsilon_M = -2$ and $\mu_M = 1$. The atomic dipole is assumed to be parallel to interface.

At first, we consider the thickness of middle slab being one wavelength. From Fig. 2, the dielectric slab supports two TE- and two TM-polarized guided modes, while the LHM slab support one TE-polarized guided mode and one TM-polarized guided mode. The surface-plasmon polariton mode cannot exist in all the dielectric, the LHM and the metal slabs for $d = \lambda$. The corresponding decay rates in such dielectric, LHM and metal slab are plotted as the function of the atomic position in Fig. 4.

From Figs. 4(a) and 4(b), it is clear that the decay rates through the guided modes exponentially decrease as the increasing of the distance between the atom and the interface and oscillate when the atom is in middle slab (see the dotted lines). Reference [13] pointed out that the total decay rate is close to $\mu_i n_i \Gamma_0$ for the dielectric slab if the thickness is large, which fits to Fig. 4(a) very well. However, from Fig. 4(b), the total decay rate of atom in the LHM slab is apparently larger and lower than $\mu_M n_M \Gamma_0$ depending on the atomic position. For the metal slab, the decay rate is zero when atom is in the middle of slab because there are evanescent fields in the metal.

Second, we consider the thickness of slab is 0.5 wavelength, where the dielectric slab supports one TE-polarized guided mode and one TM-polarized guided mode; but the LHM slab supports neither guided mode nor SPP mode (see Figs. 2 and 3). The metal slab supports two SPP modes according to Fig. 3(a). The decay rates are plotted as the function of the atomic position in Fig. 5.

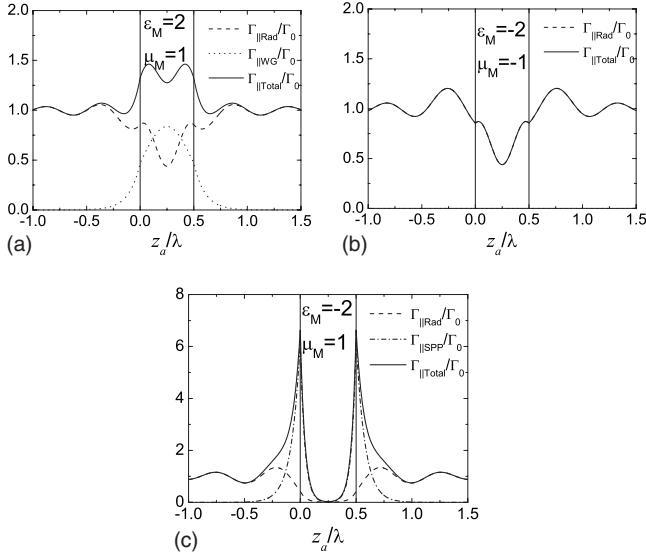


FIG. 5. The decay rates as functions of the atomic position when the thicknesses of slab are $d=0.5\lambda$ and the atomic dipole is parallel to interface. (a) The dielectric slab with $\epsilon_M=2$ and $\mu_M=1$, (b) the LHM slab with $\epsilon_M=-2$ and $\mu_M=-1$, and (c) the metal slab with $\epsilon_M=-2$ and $\mu_M=1$.

Although the number of the guided mode for the dielectric slab with $d=0.5\lambda$ is less than that for $d=\lambda$, the magnitude of the decay rate through guided mode in Fig. 5(a) does not change compared with Fig. 4(a). So there is no obvious difference between Figs. 4(a) and 5(a) except that the number of oscillation of decay rate in the slab in Fig. 5(a) is less than that in Fig. 4(a) because such number is proportional to the number of the guided mode [13]. On the contrary, there is

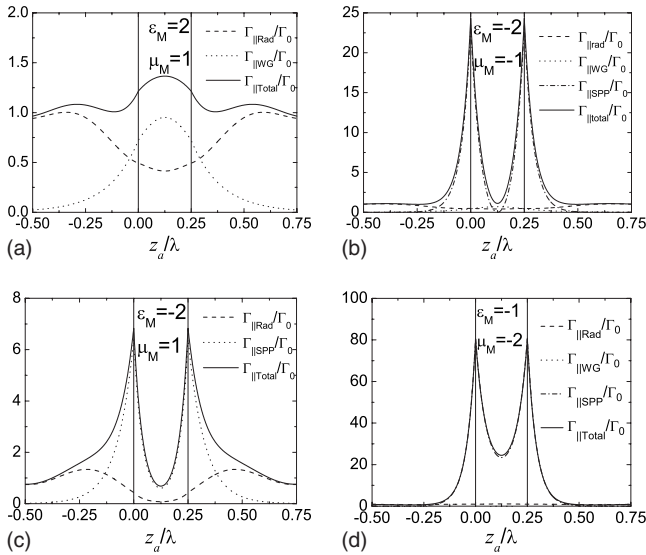


FIG. 6. The decay rates as functions of atomic position when the thicknesses of slab are $d=0.25\lambda$ and the atomic dipole is parallel to interface. (a) The dielectric slab with $\epsilon_M=2$ and $\mu_M=1$, (b) the LHM slab with $\epsilon_M=-2$ and $\mu_M=-1$, (c) the metal slab with $\epsilon_M=-2$ and $\mu_M=1$, and (d) the LHM slab with $\epsilon_M=-1$ and $\mu_M=-2$.

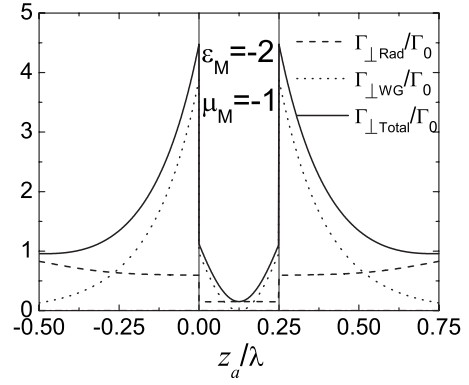


FIG. 7. The decay rates as functions of the atomic position for the LHM slab with $d=0.25\lambda$, $\epsilon_M=-2$, and $\mu_M=-1$. The atomic dipole is perpendicular to the interface.

only radiative modes for LHM slab with $d=0.5\lambda$ and consequently the total decay rate in the middle of the slab is only $0.4\Gamma_0$. In other words, the atomic decay can be deeply inhibited in a LHM slab with certain thickness though the LHM slab is transparent and has high absolute value of refractive index. For the metal slab, the decay rates near the surface are much higher because of the coupling of the atom to the SPP mode.

The decay rates for $d=0.25\lambda$ are plotted in Fig. 6. For the LHM slab with $d=0.25\lambda$, $\epsilon_M=-2$, and $\mu_M=-1$, there are the radiative mode, the guided mode, and the SPP mode. The atomic decay through the SPP modes plays the prominent role when the atom is near the surfaces of the slab, as shown in Fig. 6(b). For the corresponding metal slab, the atom near the surfaces can decay through radiative mode and SPP mode but without guided mode shown in Fig. 6(c). For $d=0.25\lambda$, the decay rate near LHM slab is much larger than that near the metal slab because the field of the SPP for the LHM slab concentrates near the surface much stronger than that for the metal slab.

Interestingly, we note that for LHM slabs with the same refractive index but different ϵ_M and μ_M , if the absolute value of permeability is larger than that of permittivity [see Fig. 6(d)], the decay rate near such slab surface is much larger than the opposite case which the absolute value of permeability is smaller than that of permittivity [see Fig.

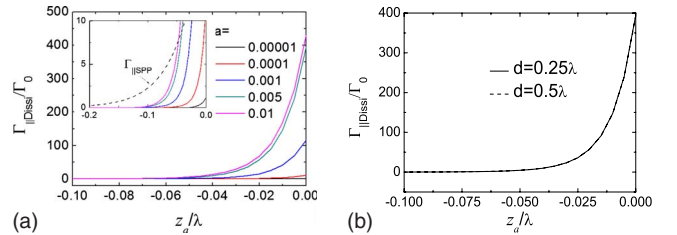


FIG. 8. (a) (Color online) For losses LHM slab with $\epsilon_M=-2 + ia$, $\mu_M=-1 + ia$, and $d=0.25\lambda$, the decay rates through dissipation $\Gamma_{||Diss}$ as functions of the atomic position for different imaginary a . (b) For losses LHM slab with $\epsilon_M=-2 + i0.005$ and $\mu_M=-1 + i0.005$, $\Gamma_{||Diss}$ as a function of the atomic position for $d=0.25\lambda$ and $d=0.5\lambda$. The atomic dipole is parallel to the interface.

6(b)]. For example, the decay rate near the surface reaches $80\Gamma_0$ for $\epsilon_M=-1$, $\mu_M=-2$ but only $25\Gamma_0$ for $\epsilon_M=-2$, $\mu_M=-1$. The main reason is that the decay rate is proportional to μ_M at the interface shown in Eqs. (11a), (16), and (20).

The case of the atomic dipole perpendicular to interface is much different from that parallel to interface. A known difference is that the decay rate for the dipole perpendicular to interface is discontinuous crossing interface due to the discontinuity of the perpendicular components of \mathbf{D} and \mathbf{B} crossing interface [13]. Here we would like to emphasize another difference between the case of the dipole perpendicular to interface and the case of the dipole parallel to interface for the LHM slab. If the LHM slab supports only TE-polarized guided mode or SPP mode, the atomic decay through the guided or the SPP modes is cancelled when the dipole is perpendicular to interface. However, for the dielectric slab, the TE-polarized guided mode almost accompany with TM-polarized guided mode; in addition there is only TM-polarized SPP mode for the metal slab. So the case of the atomic dipole perpendicular to interface is not obvious different from the case when parallel to interface for the dielectric slab and the metal slab except the discontinuous. We set $\epsilon_M=-2$, $\mu_M=-1$ and $d=0.25\lambda$; the decay rate for the dipole perpendicular to interface is shown in Fig. 7.

In this case, the LHM slab supports one TM-polarized guided mode and one TE-polarized SPP mode. As expected, there are only radiative decay and guided decay [Fig. 6(b) for the dipole parallel to interface].

B. Decay through dissipation when the LHM containing weak loss

Finally, we consider the loss of the LHM slab. Here we restrict the case of atom in the left space and near the surface (atomic position on z axis changes from -0.1λ to 0). The indexes of LHM are set as $\epsilon_M=-2+ia$, $\mu_M=-1+ia$ and $d=0.25\lambda$. The atomic dipole is parallel to interface. The total decay rate can be calculated numerically according to Eq. (10a), and the decay rate through dissipation can be defined as the difference between the total decay rate and the decay rate for the corresponding transparent slab, i.e., $\Gamma_{\parallel\text{Dissi}} = \Gamma_{\parallel\text{Total}} - \Gamma_{\parallel\text{Rad}} - \Gamma_{\parallel\text{WG}} - \Gamma_{\parallel\text{SPP}}$, where $\Gamma_{\parallel\text{Rad}}$, $\Gamma_{\parallel\text{WG}}$, and $\Gamma_{\parallel\text{SPP}}$ take the values in Fig. 6(b) approximately. The dependence of $\Gamma_{\parallel\text{Dissi}}$ on the atomic position for different imaginary parts a are plotted in Fig. 8(a). It is clear that $\Gamma_{\parallel\text{Dissi}}$ near interface decreases with the decreasing of a and becomes negligible when $z_a < -0.1\lambda$, which agree with the previous studies. The inset of Fig. 8(a) shows the comparison between the decay through SPP and decays through dissipation. It is interesting that the decay through SPP is larger than decays through dissipation when atomic position $z_a < -0.06\lambda$. The reason is that $\Gamma_{\text{SPP}} \propto \exp(-A|z_a|)$ while $\Gamma_{\text{Dissi}} \propto B/|z_a|^3$ [8,10], and $\exp(-A|z_a|)$ decreases slower than $B/|z_a|^3$ with l mathematically when l is small. However, due to $\Gamma_{\parallel\text{Rad}} \approx \Gamma_0$, $\Gamma_{\parallel\text{SPP}}$ is the largest among all channels only when $z_a \in [-0.15\lambda, -0.06\lambda]$. In Fig. 8(b), we take $\epsilon_M=-2+i0.005$, $\mu_M=-1+i0.005$ and compare $\Gamma_{\parallel\text{Dissi}}$ for $d=0.25\lambda$ (solid line) with $\Gamma_{\parallel\text{Dissi}}$ for $d=0.5\lambda$ (dashed line). It is clear that they fit to each other

very well. This result agrees with the truth that the decay through dissipation is mainly dependent on the indexes of materials and the distance but has little relation to the material's thickness. With the analysis of decay rate near the transparency LHM slab, we can distinguish the decay rate through dissipation from the total decay rate near LHM slab with little losses.

V. CONCLUSION

We analyze the atomic decay near the surface of the LHM slab in this paper at length. Both the decay through the guided mode and through surface-plasmon polariton mode are considered. We found that the atomic decay near the LHM slab has different property comparing with that near the dielectric slab and the metal slab. The unique characters of the LHM slab are: there is none of the guided mode at certain thickness for the LHM slab and it may supports both TE- and TM-polarized SPP modes. As the result, the atom near the LHM slab can decay through the radiative mode, the guided mode, and the SPP mode. If the SPP modes exist, the decay rates near the interface through SPP play the prominent role for the dipole parallel to interface. If a LHM slab supports only TE-polarized SPP mode or guided mode, the atom with the dipole moment perpendicular to interface cannot couple to these modes. Such cases disappear for the dielectric slab and the metal slab because they always support TM-polarized modes. Even if the LHM slab contains small loss, our conclusion is still valid and the decay rate through dissipation can be extracted out. Interestingly, we find that the decay through the SPP is the largest among all channels when atom is placed at an appropriate position. Our research helps to supply the content of quantum electrodynamics in LHM slab and has potential application to the single-photon source.

ACKNOWLEDGMENTS

This work is supported in part by the HKUST3/06C of HK Government, RGC of HK Government and FRG of HKBU the China Postdoctoral Science Foundation (Grant No. 20070421203 and 20081478), the National Key Project for Fundamental Research (Grant No. 2006CB921403), the Ministry of Science and Technology (Grant No. 2007CB13200), the NNSFC (Grant No. 10674103), and the Program for New Century Excellent Talents in University (Grant No. NCET-06-0384).

APPENDIX A: THE GREEN'S TENSOR IN THREE REGIONS

When the source \mathbf{r}_0 and the observe point \mathbf{r} are both in the left region, the Green's tensor is

$$\begin{aligned} \vec{G}_{LL}(\mathbf{r}, \mathbf{r}_0, \omega) = & \frac{i\mu_L(\omega)}{2(2\pi)^2} \int d^2\mathbf{K}_{\parallel} \frac{1}{K_{Lz}} e^{i\mathbf{K}_{\parallel} \cdot (\boldsymbol{\rho} - \boldsymbol{\rho}_0)} \sum_{q=e,m} \left[\{ e^{iK_{Lz}(z-z_0)} \mathbf{e}_{qL}^+ \mathbf{e}_{qL}^+ \Theta(z-z_0) + e^{-iK_{Lz}(z-z_0)} \mathbf{e}_{qL}^- \mathbf{e}_{qL}^- \Theta(z_0-z) \} \right. \\ & \left. + e^{-iK_{Lz}(z-2z_L+z_0)} \frac{r_{LM}^q + r_{MR}^q e^{2iK_{MZ}d}}{D_q} \mathbf{e}_{qL}^- \mathbf{e}_{qL}^+ \right], \end{aligned} \quad (\text{A1})$$

when the source \mathbf{r}_0 and the observe point \mathbf{r} are both in the middle region, the Green's tensor has the form of

$$\begin{aligned} \vec{G}_{MM}(\mathbf{r}, \mathbf{r}_0, \omega) = & \frac{i\mu_M(\omega)}{2(2\pi)^2} \int d^2\mathbf{K}_{\parallel} \frac{1}{K_{Mz}} \exp[i\mathbf{K}_{\parallel} \cdot (\boldsymbol{\rho} - \boldsymbol{\rho}_0)] \sum_{q=e,m} \\ & \times \left\{ \left[\mathbf{e}_{Mq}^+ e^{iK_z(z-z_0)} \Theta(z-z_0) + \frac{\mathbf{e}_{Mq}^+ r_{ML}^q r_{MR}^q e^{iK_z(z+2d_0-z_0)} + \mathbf{e}_{Mq}^- r_{MR}^q e^{iK_z(2z_R-z_0-z)}}{D_q} \right] \mathbf{e}_{Mq}^+ \right. \\ & \left. + \left[\mathbf{e}_{Mq}^- e^{-iK_z(z-z_0)} \Theta(z_0-z) + \frac{\mathbf{e}_{Mq}^+ r_{ML}^q e^{iK_z(z+z_0-2z_L)} + \mathbf{e}_{Mq}^- r_{MR}^q r_{ML}^q e^{iK_z(2d_0+z_0-z)}}{D_q} \right] \mathbf{e}_{Mq}^- \right\}. \end{aligned} \quad (\text{A2})$$

$z_L(z_R)$ is the z -coordinates of the left (right) interface of the slab. The Green's tensor for the source $\mu_L \mathbf{r}_0$ and the observe point \mathbf{r} are both in the right region which are omitted here.

In above, $\mathbf{K}_{\parallel} = K_x \hat{e}_x + K_y \hat{e}_y$, $K_{\parallel} = \sqrt{K_x^2 + K_y^2}$, $K_{L/M} = \sqrt{\varepsilon_{L/M}} \mu_{L/M} \omega / c$, and

$$\mathbf{e}_{L/Mm}^{\pm}(\mathbf{K}_{\parallel}) = \frac{1}{K_{L/M}} \left(\mp K_{L/Mz} \frac{\mathbf{K}_{\parallel}}{K_{\parallel}} + K_{\parallel} \hat{e}_z \right), \quad (\text{A3})$$

$$\mathbf{e}_{L/Me}^{\pm}(\mathbf{K}_{\parallel}) = \frac{\mathbf{K}_{\parallel}}{K_{\parallel}} \times \hat{e}_z. \quad (\text{A4})$$

APPENDIX B: THE NUMBER OF THE GUIDED MODES

Here we only take the TE mode as an example with $n_M > n_L \geq n_R$. For the guided mode, the region of K_{\parallel} is from $n_L K_0$ to $|n_M| K_0$. The condition that exists for the guided mode is that

$$D_{\text{TE}} = 1 - r_{ML}^{\text{TE}} r_{MR}^{\text{TE}} e^{2iK_{MZ}d}. \quad (\text{B1})$$

In other words,

$$\varphi = K_{MZ}d_0 + \theta_L + \theta_R = m\pi. \quad (\text{B2})$$

For right-handed material (RHM) slab M , the reflection coefficients are

$$\begin{aligned} r_{ML}^{\text{TE}} &= \frac{\mu_L K_{MZ} - i\mu_M |K_{Lz}|}{\mu_L K_{MZ} + i\mu_M |K_{Lz}|} \\ &= \frac{(\mu_L K_{MZ} - i\mu_M |K_{Lz}|)^2}{(\mu_L K_{MZ})^2 + (\mu_M |K_{Lz}|)^2} \\ &= \exp(2i\theta_L), \end{aligned} \quad (\text{B3})$$

$$\begin{aligned} r_{MR}^{\text{TE}} &= \frac{\mu_R K_{MZ} - i\mu_M |K_{Rz}|}{\mu_R K_{MZ} + i\mu_M |K_{Rz}|} \\ &= \frac{(\mu_R K_{MZ} - i\mu_M |K_{Rz}|)^2}{(\mu_R K_{MZ})^2 + (\mu_M |K_{Rz}|)^2} \\ &= \exp(2i\theta_R). \end{aligned} \quad (\text{B4})$$

In Table I, we give the values of each terms in Eq. (B2) as $K_{\parallel} = n_L$ and $K_{\parallel} = n_M K_0$ for RHM slab. Usually $K_0 d \sqrt{n_M^2 - n_L^2} > \arctan(\frac{\mu_M \sqrt{n_L^2 - n_R^2}}{\mu_R \sqrt{n_M^2 - n_L^2}})$, especially when $n_L = n_R$, we get $\arctan(\frac{\mu_M \sqrt{n_L^2 - n_R^2}}{\mu_R \sqrt{n_M^2 - n_L^2}}) = 0$. Because $\varphi(K_{\parallel} = n_L K_0) > 0$ and $\varphi(K_{\parallel} = n_M K_0) < 0$, there must be a certain K_{\parallel} leading to $\varphi = 0$ and $m = 0$. So whenever the thickness of RHM slab, there always exist at least one TE guided mode. Because φ is the decreasing function of K_{\parallel} , the number of the guided mode for RHM slab is

TABLE I. The phase φ as function of K_{\parallel} for RHM slab

K_{\parallel}	$n_L K_0$	$n_M K_0$	Monotony
$K_{MZ}d$	$K_0 d \sqrt{n_M^2 - n_L^2}$	0	Decreasing
θ_L	0	$-\pi/2$	Decreasing
θ_R	$\arctan(\mu_M \sqrt{n_L^2 - n_R^2} / \mu_R \sqrt{n_M^2 - n_L^2})$	$-\pi/2$	Decreasing
φ	$K_0 d \sqrt{n_M^2 - n_L^2} - \arctan(\mu_M \sqrt{n_L^2 - n_R^2} / \mu_R \sqrt{n_M^2 - n_L^2})$	$-\pi$	Decreasing

TABLE II. The phase φ as function of K_{\parallel} for LHM slab

K_{\parallel}	$n_L K_0$	$ n_M K_0$	Monotony
$K_{MZ}d$	$-K_0 d \sqrt{n_M^2 - n_L^2}$	0	Increasing
θ_L	0	$-\pi/2$	Decreasing
θ_R	$-\arctan(\mu_M \sqrt{n_L^2 - n_R^2} / \mu_R \sqrt{n_M^2 - n_L^2})$	$-\pi/2$	Decreasing
φ	$-K_0 d \sqrt{n_M^2 - n_L^2} - \arctan(\mu_M \sqrt{n_L^2 - n_R^2} / \mu_R \sqrt{n_M^2 - n_L^2})$	$-\pi$	Uncertain

$$N_{TE} = 1 + \left[\frac{K_0 d_0}{\pi} \sqrt{n_M^2 - n_L^2} - \frac{1}{\pi} \arctan \left(\frac{\mu_M \sqrt{n_L^2 - n_R^2}}{\mu_R \sqrt{n_M^2 - n_L^2}} \right) \right]. \quad (B5)$$

However, for LHM slab, $\varepsilon_M = -|\varepsilon_M|$, $\mu_M = -|\mu_M|$, $n_M = -|n_M|$, and $K_{MZ} = -|K_{MZ}|$,

$$\begin{aligned} r_{ML}^{TE} &= \frac{-\mu_L |K_{MZ}| + i|\mu_M| |K_{LZ}|}{-\mu_L |K_{MZ}| - i|\mu_M| |K_{LZ}|} \\ &= \frac{(-\mu_L |K_{MZ}| + i|\mu_M| |K_{LZ}|)^2}{(\mu_L |K_{MZ}|)^2 + (\mu_M |K_{LZ}|)^2} \\ &= \exp(2i\theta_L), \end{aligned} \quad (B6)$$

$$\begin{aligned} r_{MR}^{TE} &= \frac{-\mu_R |K_{MZ}| + i|\mu_M| |K_{RZ}|}{-\mu_R |K_{MZ}| - i|\mu_M| |K_{RZ}|} \\ &= \frac{(-\mu_R |K_{MZ}| + i|\mu_M| |K_{RZ}|)^2}{(\mu_R |K_{MZ}|)^2 + (\mu_M |K_{RZ}|)^2} \\ &= \exp(2i\theta_R). \end{aligned} \quad (B7)$$

In Table II, we give the values of each terms in Eq. (B2) as $K_{\parallel} = n_L$ and $K_{\parallel} = |n_M|K_0$ for LHM slab. Because both $\varphi(K_{\parallel} = n_L K_0)$ and $\varphi(K_{\parallel} = n_M K_0)$ are negative, if $|\varphi(K_{\parallel} = n_L K_0) - \varphi(K_{\parallel} = n_M K_0)| < \pi$, there may be none of the guided mode. In addition, φ is not a monotonously increasing or decreasing function of K_{\parallel} , we are unable to ascertain its maximum or minimum analytically. So the number of guided mode for the RHM is hard to get analytically. For the cases of TM-polarized mode, we can get the similar results.

-
- [1] E. M. Purcell *et al.*, Phys. Rev. **69**, 37 (1946).
[2] V. G. Veselago, Sov. Phys. Usp. **10**, 509 (1968).
[3] H. T. Dung, S. Y. Buhmann, L. Knöll, D.-G. Welsch, S. Scheel, and J. Kästel, Phys. Rev. A **68**, 043816 (2003).
[4] R. Ruppın and O. J. F. Martin, J. Chem. Phys. **121**, 11358 (2004).
[5] J. Kästel and M. Fleischhauer, Phys. Rev. A **71**, 011804(R) (2005).
[6] J. P. Xu, Y. P. Yang, N. H. Liu, and S. Y. Zhu, Eur. Phys. J. D **41**, 403 (2007).
[7] J. P. Xu, Y. P. Yang, H. Chen, and S. Y. Zhu, Phys. Rev. A **76**, 063813 (2007).
[8] Y. Yang, J. Xu, H. Chen, and S. Zhu, Phys. Rev. Lett. **100**, 043601 (2008).
[9] J. P. Xu, L. G. Wang, Y. P. Yang, Q. Lin, and S. Y. Zhu, Opt. Lett. **33**, 2005 (2008).
[10] A. Sambale, D. G. Welsch, H. T. Dung, and S. Y. Buhmann, Phys. Rev. A **78**, 053828 (2008).
[11] G. S. Agarwal, Phys. Rev. A **12**, 1475 (1975).
[12] J. M. Wylie and J. E. Sipe, Phys. Rev. A **30**, 1185 (1984).
[13] H. P. Urbach and G. L. J. A. Rikken, Phys. Rev. A **57**, 3913 (1998).
[14] R. H. Ritchie, Phys. Rev. **106**, 874 (1957).
[15] R. Ruppın, Phys. Lett. A **277**, 61 (2000).
[16] R. Ruppın, J. Phys.: Condens. Matter **13**, 1811 (2001).